Numerical Modelling of Vortex Flow Instabilities and Interactions

M. Mokry
Institute for Aerospace Research
National Research Council, Ottawa, Canada, K1A 0R6

Abstract

Evolution of vortices and their interactions are investigated in the Lagrangian context using the continuous vortex sheet method. Among the topics investigated are the numerical Helmholtz instability on a circular vortex sheet, the fractal-pattern instability on an expanding vortex spiral, interactions of vortices with shear layers, and some other phenomena related to experimental observations in the laboratory and nature.

Nomenclature

a,b	Fourier coefficients
C	oriented contour
f	Cauchy density
h	width of constant-density segment
i	imaginary unit, $\sqrt{-1}$
k	positive integer
n	number of segments of C
q	velocity
u,v	velocity components
w	complex velocity
x,y	Cartesian coordinates
z	complex coordinate of observation point
Γ	spanwise circulation
γ	vortex density
δ	Dirac delta function
ρ	radius, wing half-span
ν	angle between real axis and normal to C
τ	pseudo-time
ζ	complex coordinate of running point

Subscripts
n	normal
t	tangential

Superscripts
$+$	to the left of C
$-$	to the right of C
$*$	complex conjugation

Report Documentation Page

1. REPORT DATE	2. REPORT TYPE	3. DATES COVERED
00 MAR 2003	**N/A**	**-**

4. TITLE AND SUBTITLE	5a. CONTRACT NUMBER
Numicerial Modelling of Vortex Flow Instabilities and Interactions	5b. GRANT NUMBER
	5c. PROGRAM ELEMENT NUMBER

6. AUTHOR(S)	5d. PROJECT NUMBER
	5e. TASK NUMBER
	5f. WORK UNIT NUMBER

7. PERFORMING ORGANIZATION NAME(S) AND ADDRESS(ES)	8. PERFORMING ORGANIZATION REPORT NUMBER
NATO Research and Technology Organisation BP 25, 7 Rue Ancelle, F-92201 Neuilly-Sue-Seine Cedex, France	

9. SPONSORING/MONITORING AGENCY NAME(S) AND ADDRESS(ES)	10. SPONSOR/MONITOR'S ACRONYM(S)
	11. SPONSOR/MONITOR'S REPORT NUMBER(S)

12. DISTRIBUTION/AVAILABILITY STATEMENT
Approved for public release, distribution unlimited

13. SUPPLEMENTARY NOTES
Also see: ADM001490, Presented at RTO Applied Vehicle Technology Panel (AVT) Symposium held inLeon, Norway on 7-11 May 2001, The original document contains color images.

14. ABSTRACT

15. SUBJECT TERMS

16. SECURITY CLASSIFICATION OF:			17. LIMITATION OF ABSTRACT	18. NUMBER OF PAGES	19a. NAME OF RESPONSIBLE PERSON
a. REPORT **unclassified**	b. ABSTRACT **unclassified**	c. THIS PAGE **unclassified**	**UU**	**12**	

Introduction

This paper studies some fundamentals, although in a simplified form, of the formation and evolution of vortices. The starting point is a two-dimensional vortex sheet along which the fluid velocity is discontinuous. A global characteristic of the vortex sheet evolution is stretching, implying that the vortex density (strength) of the sheet is a decreasing function of time. Locally, there may be short-lived contractions of the sheet in which strength increases sharply, preceding sudden qualitative changes such as the onset of roll-up and instabilities.

The majority of present-day vortex methods have evolved from the point-vortex approximation by Rosenhead [1]. A schematic of such a scheme is shown in Fig.1. The vortex particles, which are created at the solid boundary at each time step, in order to satisfy the no-slip boundary condition, are freed in the subsequent time steps to move with the flow and diffuse [2]. However, in order for the numerical simulation to be accurate, the particles must, to a certain degree, be uniformly distributed. This requires the usage of techniques such as redistribution, splitting and merging of particles [3]. Results obtained in this way are equivalent to gridless solutions of the incompressible-flow Navier-Stokes equations.

The continuous vortex sheet method [4] employed in this paper is relatively simple in comparison, but does not have the capabilities of creating or diffusing vorticity (or no attempt has been made so far). It does, however, model the jump discontinuity across of thin vortex sheets, Fig.2, preserving discrete spiral structures of vortices similar to those observed in flow visualizations [5].
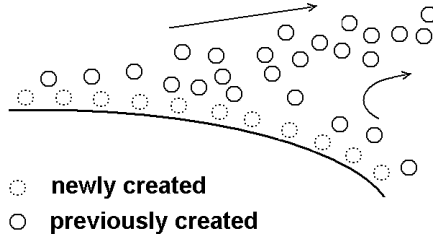

Fig.1   Discrete vortex representation
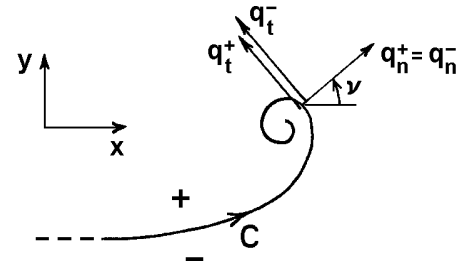   (after Leonard [2])

Fig.2   Continuous vortex sheet
         representation

Continuous sheet model

The complex velocity induced by an oriented vortex sheet C at an observation point z is

$$w(z) = \int_C \frac{i\gamma(\zeta)}{2\pi(\zeta - z)} |d\zeta| = \frac{1}{2\pi i}\int_C \frac{f(\zeta)}{\zeta - z}d\zeta \tag{1}$$

where ζ is a point on C and γ is the real-valued vortex density function. The complex contour element $d\zeta$ can be expressed in terms of the arc length element $|d\zeta|$ as

$$d\zeta = |d\zeta| i e^{i\nu(\zeta)}$$

where ν is the angle between the real axis and the normal to C, pointing to the right, see Fig.2. Accordingly, the complex density function in Eq.(1) is given by

$$f(\zeta) = i\gamma(\zeta)e^{-i\nu(\zeta)} \tag{2}$$

The second integral of Eq.(1), also known as the Cauchy-type integral, describes a function, which is analytic everywhere except across C. In accordance with the Plemelj formula,

$$w^+(\zeta) - w^-(\zeta) = f(\zeta)$$
(3)

where the superscripts $+$ and $-$ denote the limiting values of w to the left and right of C respectively. If z is a point on C, the complex velocity is calculated by taking the principal value of the Cauchy-type integral in Eq.(1). Expressing the complex velocity on C in terms of the normal and tangential components,

$$w(\zeta) = [q_n(\zeta) - iq_t(\zeta)]e^{-iv(\zeta)}$$
(4)

it follows, from Eqs.(2)-(4),

$$q_n^+(\zeta) - q_n^-(\zeta) = 0$$

and

$$q_t^+(\zeta) - q_t^-(\zeta) = -\gamma(\zeta)$$
(5)

The self-induced time evolution of C is calculated by integrating

$$\frac{dz}{d\tau} = w^*(z)$$
(6)

where the term on the right-hand side is the complex conjugate of the principal value of Eq.(1).

The integration is implemented by dividing the contour into n straight-line segments (panels) of constant vortex density, and advancing the solution in finite steps of the (pseudo-)time τ. From Eq.(1) it follows that if γ is chosen to be non-dimensional, then also w is non-dimensional and, from Eq.(6), τ must have the same dimension as z (usually normalized by span). Conservation of vorticity implies

$$\gamma(\zeta)|d\zeta| = \text{constant}$$

Accordingly, if a vortex segment stretches, its density decreases and if it contracts, its density increases. A detailed description of the numerical algorithm is given in Ref.[4].

Vorticity circuits

As an example we consider C to be the circle of radius ρ:

$$\zeta = \rho\, e^{iv}$$
(7)

A variety of vortex flows can be generated by prescribing the vortex density as the Fourier series

$$\gamma(v) = 0.5a_0 + \sum_{j \geq 1}(a_j \cos jv + b_j \sin jv)$$

where $\gamma(v)$ is to be interpreted as $\gamma(v(\zeta))$.

Two elementary cases will be analyzed here: 1) a cylindrical volume of fluid moving in fluid at rest and, 2) a cylindrical volume of fluid at rest around which fluid circulates.

The first case is obtained by choosing

$$\gamma(v) = a_1 \cos v = \frac{a_1}{2}(e^{iv} + e^{-iv})$$
(8)

From Eqs.(2) and (7)

$$f(\zeta) = i\frac{a_1}{2}\left[1 + \left(\frac{\rho}{\zeta}\right)^2\right]$$

Substituting in Eq.(1) and using the Cauchy formula it follows

$$w(z) = i\frac{a_1}{2}\left(\frac{1}{2\pi i}\int_C \frac{1}{\zeta - z}d\zeta + \frac{1}{2\pi i}\int_C \frac{(\rho/\zeta)^2}{\zeta - z}d\zeta\right) = \begin{cases} i\dfrac{a_1}{2}, & |z| < \rho \\ -i\dfrac{a_1}{2}\dfrac{\rho^2}{z^2}, & |z| > \rho \end{cases}$$

This result can be interpreted as follows: inside the circle, there is a uniform downward motion described by the velocity components

$$u = 0 \quad \text{and} \quad v = -0.5a_1$$

Outside the circle, the velocity is that of a point doublet of strength $\pi a_1 \rho^2$, oriented in the vertical direction. It describes the velocity of ambient fluid displaced by the moving cylinder.

The evolution of the vortex circuit whose initial conditions are given by Eqs.(7)-(8) is shown in Fig.3. The left-hand figure column shows the changes of the circuit geometry and the right-hand column is the corresponding histogram of γ in the 50% reduced length scale. It is seen that the circle deforms smoothly until $\tau = 0.72$ (normalized by diameter). At that instant two density peaks occur, followed by the onset of two lee-side rollups. The sudden appearance of singularities (infinite-curvature points) in the shape of an evolving vortex sheet is a phenomenon well explored theoretically [6][7]. The subsequent evolution of the vortex circuit in Fig.3 is as expected: a continuous stretching driven by the two roll-ups.

The second example is obtained by choosing

$$\gamma(v) = 0.5a_0 = \text{constant} \tag{9}$$

From Eqs.(2) and (7)

$$f(\zeta) = i\frac{a_0}{2}\frac{\rho}{\zeta}$$

and from Eq.(1)

$$w(z) = i\frac{a_0}{2}\frac{1}{2\pi i}\int_C \frac{\rho/\zeta}{\zeta - z}d\zeta = \begin{cases} 0, & |z| < \rho \\ -i\dfrac{a_0}{2}\dfrac{\rho}{z}, & |z| > \rho \end{cases}$$

Inside the circle, there is no flow. Outside, the flow field is identical with that generated by a point vortex of strength $\pi a_0 \rho$, located at the centre of the circle. Since

$$q_t^+ = 0$$

it follows from Eqs.(5) and (9)

$$q_t^- = 0.5a_0$$

The circumference of the circle turns with the average of the above velocities (principal value):

$$q_t = 0.5(q_t^+ + q_t^-) = 0.25a_0$$

As may be conjectured from Fig.4, the circle keeps turning, with flow swirling around twice as fast, until about $\tau = 4$. At this (critical) time the accumulated numerical errors have already created noticeable wiggles in the shape of the circle and small variations of γ appear. Subsequently, a rapid breakdown of the vortex sheet takes place: multiple peaks of γ pop up, followed by a series of roll-ups on the circle circumference, which are accompanied by an intensive stretching. The observed long-term existence of a slightly perturbed equilibrium solution, terminated by a sudden transition, is consistent with the theoretical analyses [8].

The difference between the two cases shown can be summarized as follows. The variation of γ in Fig.3 allows a creation of density peaks early in the vortex evolution process, enabling two orderly roll-ups that facilitate vortex sheet stretching. In Fig.4, because of the circular shape of C and γ = constant, the natural stretching is suppressed – until the Helmholtz instability takes over.
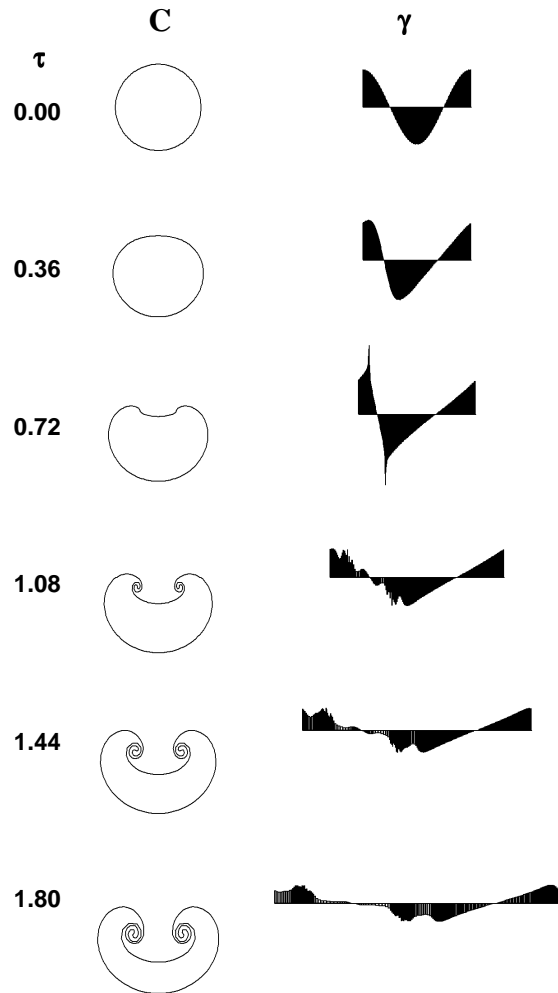
Fig.3   Evolution of vorticity circuit,
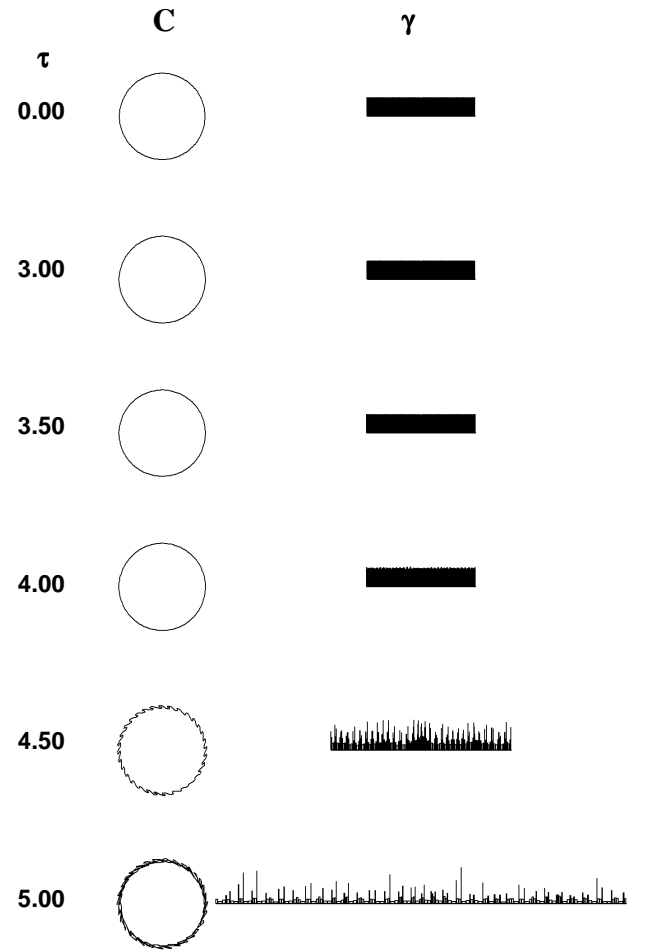$\gamma = \cos \nu$, $n = 180$; $\Delta \tau = 0.02$

Fig.4   Evolution of vorticity circuit,
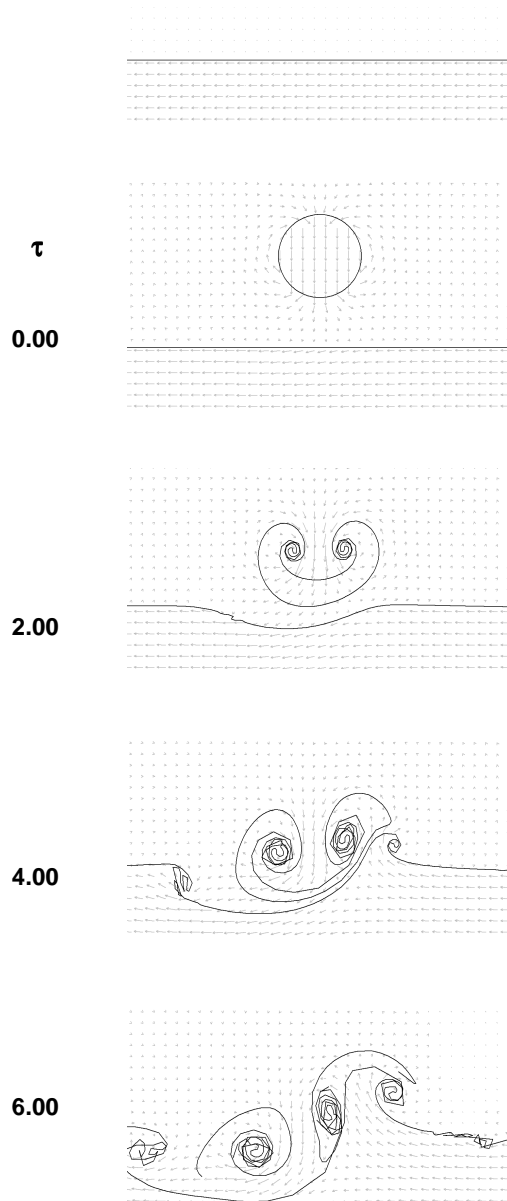$\gamma = 0.5$, $n = 180$; $\Delta \tau = 0.02$

Fig.5 Interaction of vorticity circuit $\gamma = \cos\nu$, $n = 180$ and shear layer, $\gamma = -0.4$, in crosswind, $u = -0.2$; $\Delta\tau = 0.02$
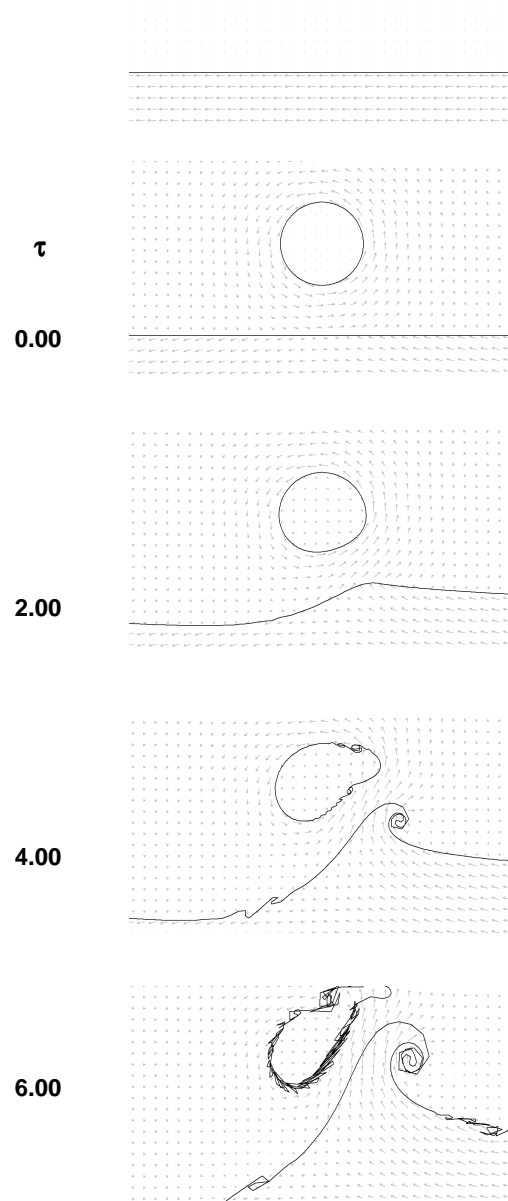
Fig.6 Interaction of vorticity circuit $\gamma = 0.5$, $n = 180$ and shear layer, $\gamma = -0.4$, in crosswind, $u = -0.2$; $\Delta\tau = 0.02$

Interactions

Vortex sheet roll-up can be also induced externally, for example by an interaction of several vortex sheets. In the first frame of Fig.5 we show a straight vortex sheet of constant density. It is combined with a constant crosswind in such a way that there is no flow above the sheet and flow to the left below. If isolated, the sheet would eventually be subject to a Helhmholtz instability similar to that developed on the circle in Fig.4.

However, this situation changes when a vorticity circuit, similar to that shown in Fig.3, is implanted (at time $\tau = 0$). The circuit moves down into the vortex sheet, first indenting it and then inducing vortices at the edges of the indentation basin. The interaction is not symmetrical because one of the impinging circuit's vortices is of the same sign as the straight vortex sheet whereas the other is of opposite sign. This flow pattern resembles the interaction of the counter-rotating aircraft vortices with an atmospheric shear layer.

The example in Fig.6 is perhaps even more interesting because it combines the same vortex sheet, with no flow above, with a vorticity circuit of Fig.4, with no translation motion of its own. It is the circulation around the vortex circuit that initializes the interaction: the straight vortex sheet is pushed down on the left and pulled up on the right. The deformed vortex sheet no longer provides zero flow above and thus interacts with the vorticity circuit. Since in this case the induced shear layer vortex on the right rotates flow in the direction opposite to that of the vortex circuit, both systems rise. A similar effect can be also detected in Fig.5. The couple of equally oriented vortices on the left have a tendency to rotate about each other but the couple of oppositely oriented vortices on the right translate upwards.

Vorticity lines

Besides the vorticity circuits it is also of interest to investigate finite-length stretches of vorticity. Most familiar are the trailing vortex sheets of lifting wings, known to roll up into counter-rotating wing tip vortices. In essence, the integrals of Eq.(1) are singular at the ends of an open contour C, providing nuclei of roll-up, unless the vortex density is vanishing there. Here we shall consider a vortex segment parallel to the x-axis, having a "bell-shaped" density distribution

$$\gamma(x) = \frac{k}{\sqrt{\pi}} \exp(-k^2 x^2) \tag{10}$$

where k is a positive integer. It can be shown that

$$\int_{-\infty}^{\infty} \gamma(x) dx = 1$$

and

$$\lim_{k \to \infty} \gamma(x) = \delta(x)$$

where δ is the Dirac delta function. In Fig.7, we immediately notice that the peaking of γ during the vortex sheet evolution does not follow the limiting process $k \to \infty$. Although the condition of constant area under the γ curve is satisfied by conservation of vorticity, the base does not narrow when peaking occurs, leading to a "thorn-like" γ distribution. In any case, it would be unrealistic to expect that a cumulative (singular) vorticity could be generated during a spontaneous vortex evolution process.

The case shown in Fig.8 is obtained by cutting the vortex segment in half and inserting a segment of width h, having the constant density

$$\gamma(x) = \frac{k}{\sqrt{\pi}}, \qquad |x| \leq h/2 \tag{11}$$

On the left and right flanks thus

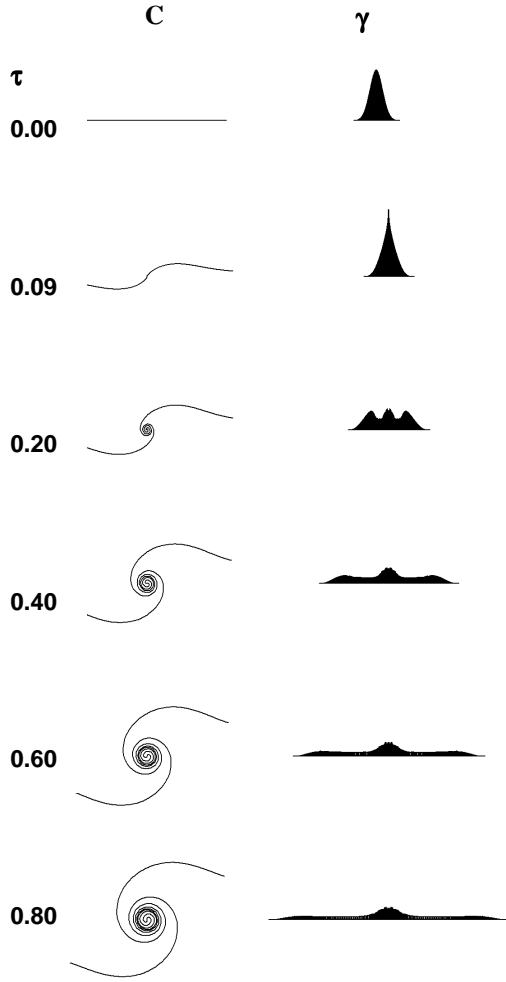$$\gamma(x) = \frac{k}{\sqrt{\pi}} \exp[-k^2 (|x| - h/2)^2], \qquad |x| > h/2 \tag{12}$$

Fig.7   Evolution of vortex segment, type **Sa,**
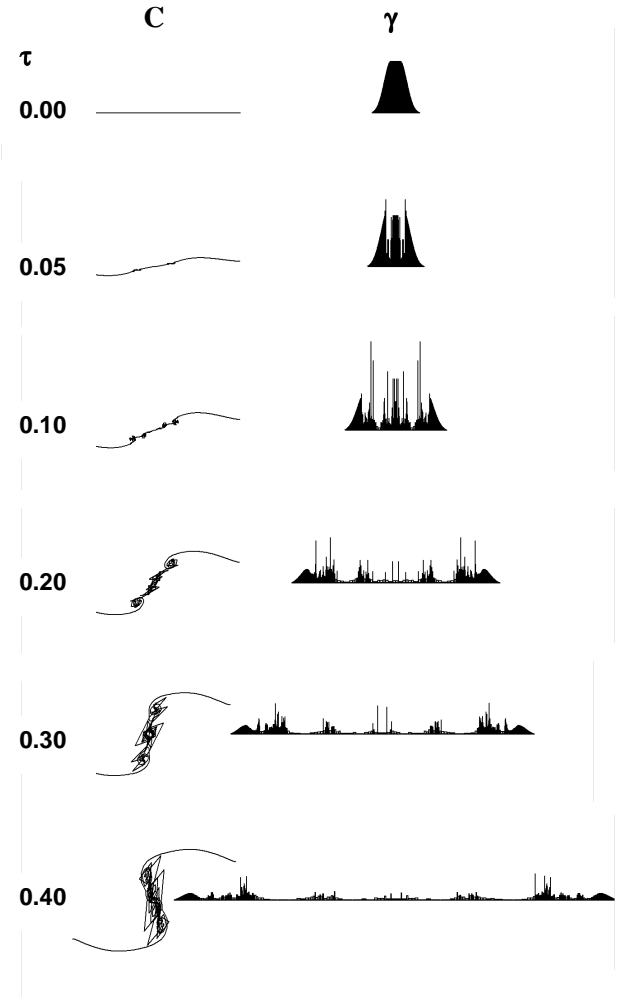Eq.(10), $k = 5$, $n = 240$; $\Delta\tau = 0.002$

Fig.8   Evolution of vortex segment, type **SBa**,
Eqs.(11) and (12), $k = 5$, $h = 0.2$, $n = 240$;
$\Delta\tau = 0.001$

The γ distribution described by Eqs.(11) and (12) is still continuously differentiable, but the impact of this modification is startling. As may be observed in Fig.8, the peaking takes place at the ends of the constant-density interval and later spreads to several locations in between. Compared to the smooth roll-up in Fig.7, the evolution of the constant-density segment in Fig.8 is "noisy", displaying Helmholtz-type instabilities.

Although the real-world phenomena have more than two-dimensions and the underlying physics is much different, similar vortex patterns are also observed on a grand scale as hurricanes, Fig.9, or galaxies, Fig.10. Edwin Hubble classified the regular galaxies into three major types: spiral (S), barred spiral (SB), and elliptical (E), as shown in the diagram of Fig.11. Spiral galaxies have a bulge at the centre and a disk containing spiral arms. Barred spiral galaxies are spirals that have a bar running across the center of the galaxy. Elliptical galaxies do not have a disk or arms and the stars within move irregularly [9]. Just how the different types are established is believed to be a matter of initial conditions of the amount of mass and angular momentum in the condensing gas cloud, and of interacting with nearby galaxies [10]. By Hubble's classification, the computer simulation in Fig.7 would be of type Sa and that in Fig.8 of type SBa.

Fig.9   Hurricane Fran, Sept.4, 1996,
             (NOAA / NASA)

Fig.10   Whirlpool Galaxy (M 51/NGC 5194),
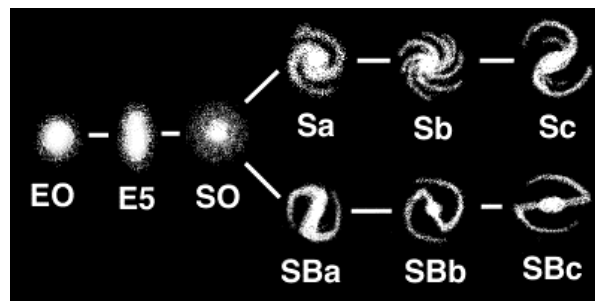   C. Messier (1773) / P. Mechain (1781)

Fig.11   Hubble's Tuning Fork Diagram

Vortex spirals

The stretching of the vortex sheet, as it winds into a spiral, is known to have a stabilizing effect [11], [12]. Locally, the stability of this convection problem can be characterized by the displacement of the vortex segment relative to its size (Courant number)

$$|w| \frac{\Delta \tau}{|\Delta \zeta|}$$

When using a constant time stepping, initially an unstable behaviour may be observed. Eventually, the spiral stabilizes because $|\Delta \zeta|$ increases due to stretching.

The four examples in Fig.12 were obtained for a trailing sheet behind an elliptically-loaded wing, represented by the lifting line with the spanwise circulation

$$\Gamma(x) = (\rho^2 - x^2)^{1/2}, \quad |x| \le \rho$$

where ρ is the half span. The (non-dimensional) vortex density distribution is obtained as

$$\gamma(x) = -\frac{d\Gamma(x)}{dx} = (x/\rho)[1 - (x/\rho)^2]^{-1/2}$$

Since the magnitude of γ grows asymptotically towards the wing tips, the segment endpoints have been distributed as

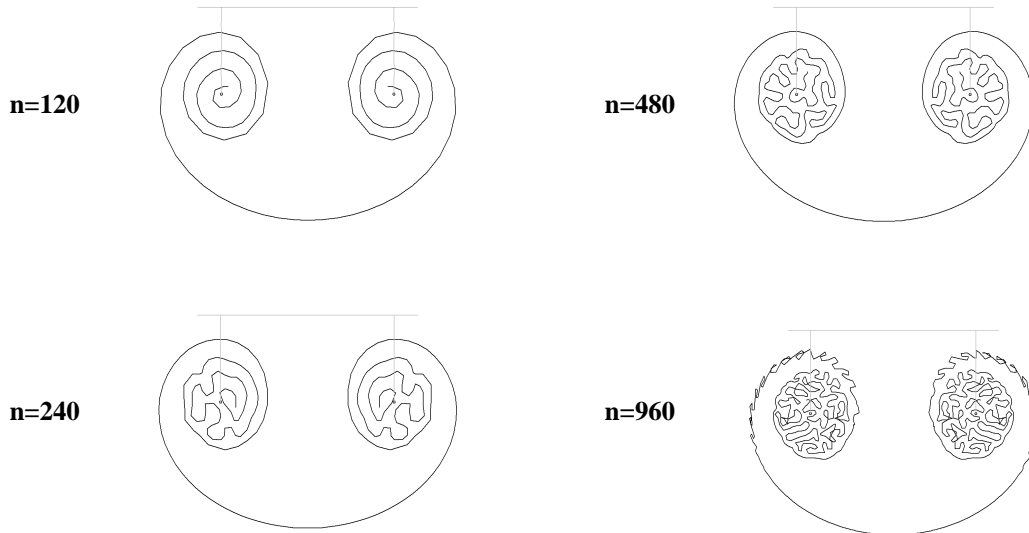$$x_j / \rho = -\cos(\pi j / n), \quad 0 \le j \le n$$

Fig.12   Numerical instability of the near-field vortex-sheet spiral,
$\Delta \tau = 0.02$, 100 steps

All the spirals shown in Fig.12 were obtained after 100 steps using a constant pseudo-time step $\Delta \tau = 0.02$ (normalized by wing span). The spiral built of 120 segments appears to be most stable. The small-scale undulations, developed in the very early stage of the roll-up, smooth out. The spirals with a more refined segmenting develop a chaos-like labyrinth pattern that persists in the later stages of their development. This

phenomenon is also known as the fractalization by folding [13]. Although the fractal curve of Koch is often used as an example, the folds of the spiral relate more closely to the curve of Peano [14]. The latter curve is described by a continuous function of the arc length that fills a bounded planar domain (rectangle) and in the limit of infinite refinement has nowhere a derivative [15]. The labyrinth pattern obtained inside the spiral of Fig.13 describes a vortex core to the extent the formulation by Eq.(1) permits: the tangential velocity decreases toward the core centre like in viscous flow and it is difficult to distinguish the individual winds of the spiral.

It is worth noting that undulations of the spiral arm similar to those shown in Fig.13 have been observed experimentally by Pierce [16], in airflow around plates accelerated from rest, see Fig.14. Evidently, there is a relationship between real physics and the computer simulation. As may be expected, the connection between the artificial viscosity introduced by the finite time stepping and true viscosity holds the clue.
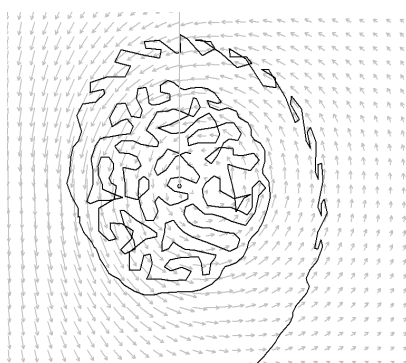
Fig.13 Velocity field of a fractal vortex spiral
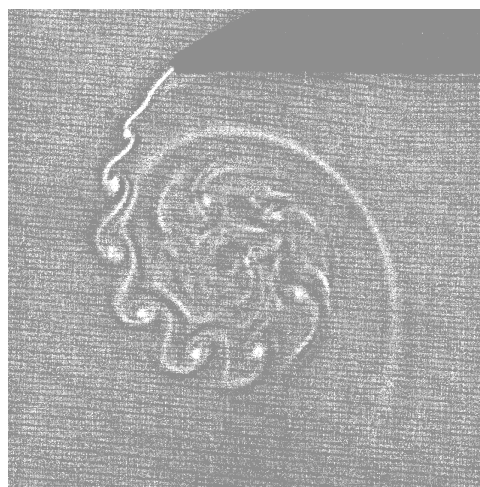(detail of Fig.12, case $n = 960$)

Fig.14 Vortex sheet roll-up behind a plate with a convex front surface and flat rear surface.
Reprinted from the article by Pierce [16] with the permission of Cambridge University Press.

Concluding remarks

It has been shown that a number of physical phenomena related to the evolution of vortices, such as stretching, contraction, instabilities and interactions, can be modeled in a simplified form by the continuous sheet method. The numerical examples given in this paper were produced by a code VSR (for Vortex Sheet Roll-up), written in Visual C++ as a Windows application.

References

[1] Rosenhead, L. (1931) The formation of vortices from a surface of discontinuity. *Phys. Fluids* **A 5,** 170-192.

[2] Leonard, A. (1980) Vortex methods for flow simulation. *J.Comp.Phys* **37**, 289-335.

[3] Leonard, A., Shields, D., Salmon, J.K., Winckelmans, G.S., and Ploumhans, P. (1997) Recent advances in high resolution vortex methods for incompressible flows. *AIAA 97-2108*.

[4] Mokry, M. and Yeung, A.F.K. (1999) On the evolution of trailing vortex sheets. *ESAIM Proc.* **7**, 292-303, http://www.emath.fr/proc/Vol.7/

[5] Van Dyke, M. (1982) *An album of fluid motion.* Parabolic Press, Stanford, 42-59.

[6] Moore, D. W. (1978) The spontaneous appearance of a singularity in the shape of an evolving vortex sheet. *Proc.R.Soc.Lond.* **A 365** , 105-119.

[7] Caflisch, R. E. and Orellana, O.F. (1989) Singular solutions and ill-posedness for the evolution of vortex sheets. *SIAM J.Math.Anal.* **20**, 293-307.

[8] Caflisch, R.E. and Orellana, O.F. (1986) Long time existence for slightly perturbed vortex sheet. *Comm.Pure Appl.Math.* **39** 807-838.

[9] http://amazing-space.stsci.edu/

[10] Friedman, H. (1998) *The astronomer's universe*. Norton & Com., 229-231.

[11] Moore, D.W. and Griffith-Jones, R. (1974) The stability of an expanding circular vortex sheet. *Mathematika* **21**, 128-133.

[12] Moore, D.W (1976) The stability of an evolving two-dimensional vortex sheet. *Mathematika* **23**, 35-44.

[13] Chorin, A.J. (1994) *Vorticity and turbulence.* Springer-Verlag, 99-101.

[14] Peano, G. (1890) Sur une courbe, qui remplit toute une aire plane. *Math. Annalen* **36**, 157-160.

[15] Hairer, E. and Wanner, G. (1997) *Analysis by its history*, 2nd ed. Springer-Verlag, 263-270 and 290-298.

[16] Pierce, D. (1961) Photographic evidence of the formation and growth of vorticity behind plates accelerated from rest in still air. *J.Fluid Mech.* **11**, 460-473.